

*Short communication*

## **Towards an Efficient Direct Glucose Anion Exchange Membrane Fuel Cell System with Several Electro-Oxidation Units**

*Spets Jukka-Pekka<sup>1\*</sup>, Kanninen Petri<sup>2</sup>, Kallio Tanja<sup>2</sup>, Selkäinaho Jorma<sup>3</sup>, Kiros Yohannes<sup>4</sup>, Saari Kari<sup>1</sup>, Larmi Martti<sup>1</sup>*

<sup>1</sup> Dept. Mechanical Engineering, School of Engineering, Aalto University, Espoo, P.O. Box 14400, FI-00076 Aalto, Finland

<sup>2</sup> Dept. Chemistry and Material Science, School of Chemical Engineering, Aalto University, Espoo, P.O. Box 16100, FI-00076 Aalto, Finland

<sup>3</sup> Dept. Electrical Engineering and Automation, School of Electrical Engineering, Aalto University, Espoo, P.O. Box 15500, FI-00076 Aalto, Finland

<sup>4</sup> Dept. Chemical Engineering and Technology, KTH Royal Institute of Technology, SE-100 44 Stockholm, Sweden

\*E-mail: [jukka-pekka.spets@aalto.fi](mailto:jukka-pekka.spets@aalto.fi)

*Received:* 13 February 2017 / *Accepted:* 19 March 2017 / *Published:* 12 April 2017

---

This work covers the direct glucose anion exchange membrane fuel cell (AEMFC) with near-neutral-state electrolyte of 0.1 M [PO<sub>4</sub>]<sub>tot</sub> having two high-performing anode electrocatalysts (Pt and PtNi) at 37 °C and at a glucose concentration of 0.1 M. The cathode catalyst in each test was a Pt supported on carbon (60 wt.%). The PtNi/C had a total metal content of 40 wt.% and the Pt/C 60 wt.%. The operation of the AEMFC was controlled by means of an in-house made electronic load with PI-controller (i.e. a feedback controller, which has proportional and integral action on control error signal). There were two primary objectives with this study. At first, to find out how the electrode modifications of the anode (i.e. by increasing the thicknesses of these electrodes by adding extra carbon) affect the Coulombic efficiency (CE, based on the exchange of two electrons) and the specific energy (SPE, Wh kg<sup>-1</sup>) values of the direct glucose AEMFC. Secondly, investigate how a two-stage fuel cell system with two fuel cells concatenated and used one after the other for the electrochemical oxidation of glucose, influence the CE and SPE values. The results show that the modified PtNi anode shows superior results for the AEMFC compared to our earlier results. As for the two-stage fuel cell system, it increased the average electric power (mWh) and SPE when compared to single fuel cell systems except when the higher selective anode catalyst (Pt) was used in the first fuel cell prior to the fuel cell in the second fuel cell containing the lower selective anode catalyst (PtNi).

---

**Keywords:** glucose, anode electrocatalysts, anion exchange membrane fuel cell, near-neutral-state electrolyte, multistage fuel cell system

## 1. INTRODUCTION

So far the electrochemical oxidation of glucose has occurred with at most two electron transfer in different fuel cells, when the maximum number of the available electrons is 24 per one glucose molecule [1-3]. Our reported tests with both the direct glucose cylinder and the rectangular (flat) type anion exchange membrane fuel cells (AEMFC) confirm previous results that at the most only two electrons are extracted during electrochemical oxidation of glucose in a near-neutral-state electrolyte [4-6]. Thus, it has to be admitted that a single fuel cell with a certain anode – cathode pair is ineffective for achieving a high degree of oxidation of glucose, which can theoretically provide the transfer of 24 electrons per molecule. This is due to facts that the used anode catalysts are either unselective towards the oxidation products of glucose or these catalysts are being poisoned by these oxidation products [7-8]. In this work, we continue the research on the direct glucose AEMFC from the point of view of our earlier reported studies [6]. At first, we describe the optimization of the Pt and PtNi as anodes for the oxidation of glucose and as assembled further in the AEMFC. Then, we report the tests with an AEMFC system with two separate electro-oxidation units in series. Early reported works on the multistage structures of the fuel cells systems are related e.g. to multi-stack structures of several microbial fuel cells (MFCs) for the different bioorganic fuels [9] or to solid oxide fuel cells (SOFCs) for the hydrogen, methane and carbon monoxide gases as fuels [10]. Based on the literature and patent searches, it is suggested that our proposed two-stage direct glucose AEMFC system, in which the oxidation reaction are occurring in the separate stages, contains novelty value when compared to these early reported works [9,10].

## 2. EXPERIMENTAL

### 2.1 The test equipment

#### 2.1.1 Main device

The main equipment that were applied in this work are shown in Fig. 1.

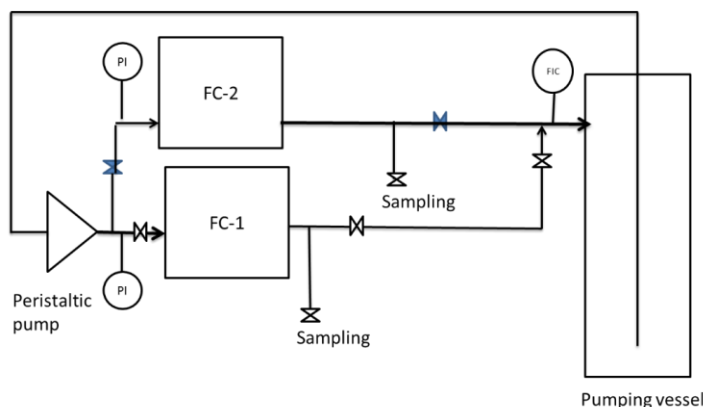


**Figure 1.** Schematic and units of the two-stage fuel cell system.

The main equipment were similar to the devices in our previous work [6] except for the second added test fuel cell equipment. Electronic devices and connections including the PI controller for the electronic load and the TIC controller for heating the electrodes of the fuel cells were also analogous as were used earlier in the single fuel cell [6]. The voltage and current values were measured and recorded similarly as in our earlier published research [6].

### 2.1.2 Preparation of the electrodes

Fuel cell electrodes were prepared as described earlier [6]. In brief, carbon supported Pt (60 wt.%, by Alfa Aesar, marked as Pt(60)) and PtNi (1:6, 40 wt.%, by Premetek, abbreviated as PtNi(40)) were used as the anode catalysts and Pt (60 wt.%, by Alfa Aesar, abbreviated as Pt(60)) as the cathode catalyst. Carbon black (Vulcan XC-72, Cabot Corp.) was added to the anode catalysts to increase the anode thickness so that the metal content of the catalyst powder was kept at 10 wt.%. The catalysts were mixed with distilled water, isopropanol and FAA3 ionomer solution (Fumatech) by magnetic stirring and sonication. The resulting inks were sprayed with an airbrush on hydrophilic ELAT-H carbon cloth (NuVant Systems) in the case of anode catalysts and on hydrophobic GDL-CT carbon cloth (FuelCellsEtc) in the case of cathode catalysts. Finally, the electrodes were dried in a vacuum oven at 40°C. The metal loadings of the anodes are presented in Table 1 and the cathode Pt loading was  $3.1 \pm 0.1 \text{ mg cm}^{-2}$ .

The resulting thicknesses of the anodes PtNi(40)+C and Pt(60)+C were measured to be 920  $\mu\text{m}$  and 950  $\mu\text{m}$ , respectively. The thickness of the cathode electrodes were 500  $\mu\text{m}$ . The geometrical areas of the electrodes in the rectangular (flat) fuel cell were 5  $\text{cm}^2$ .

**Table 1.** The anode catalysts and their respective mass loadings.

Anode catalyst (wt.%)	Carbon support type	Manufacturer	Total mass loading [ $\text{mg cm}^{-2}$ ]
Pt(60) + C	activated carbon	Alfa Aesar	1.63
PtNi(1:6, 40) + C	Vulcan XC-72	Premetek	1.57

### 2.1.3. The gaskets of the test fuel cell

Due to the increased thicknesses of the PtNi(40)+C (920  $\mu\text{m}$ ) and Pt(60)+C (950  $\mu\text{m}$ ) anodes, two pieces of nitrile rubbers were used on the anode side. On the cathode side PTFE and a rubber gasket were similar as in our earlier work in [6].

### 2.1.4 Electronic load with PI-controller (ELPI)

The electric power load has been designed for small currents. The current is measured by using a 10 ohm resistor. The voltage over this resistor reduces the control voltage that comes from the microcontroller.

## 2.2. The test procedure

The preparation procedures were equal as they were in our earlier work [6]. Glucose and potassium dihydrogen phosphate ( $\text{KH}_2\text{PO}_4$ , Sigma-Aldrich) were dissolved in distilled water. The concentrations of both compounds were 0.1 M. The pH value was set at 7.4 by adding potassium hydroxide (KOH, Alcol) in the aqueous solution, which contained glucose and  $\text{KH}_2\text{PO}_4$ . The volumes of the fuel-electrolyte solutions in the feeds were  $0.11 \text{ dm}^3$  in all the tests, except for  $0.1 \text{ dm}^3$  in the test with a single fuel cell with PtNi(40)+C as the anode.

The fuel-electrolyte solution was pumped to the anode of the first fuel cell, in which the electrodes were electrically heated and maintained at  $37^\circ\text{C}$  by the TIC controller. The measurements of the polarization curves were conducted as in [6]. While measuring the current-voltage values of the two-stage fuel cell system, the open circuit voltage (OCV) generation was recorded for a duration of one hour until a minimal variation of  $200 \mu\text{V min}^{-1}$  in both fuel cells was obtained. After this the Coulombic efficiency over time (i.e. the current-voltage test) was recorded as follows: at the start the current values were set by the PI-controller (in constant voltage (CV) mode) of the electronic load to values in order of the maximum current density  $20\text{-}50 \mu\text{A cm}^{-2}$  for each anode-cathode pair (i.e. current values between 100 and 250  $\mu\text{A}$ ). The first test fuel cell was used for 16.8 to 19.2 hours. Then the fuel-electrolyte solution was fed to the second fuel cell. After OCV generation for one hour, the current was taken in values between 100 to 250  $\mu\text{A}$  until the fuel cell operation was stopped due to mass transfer limitations, which took place as reported in our earlier work with the single direct glucose AEMFC [6]. Because the knob of the PI controller had reverse direction for increasing the control boosting (for constant current mode CC as clockwise and for CV as counter clockwise), the control capacity in CV mode run had to be regenerated at maximum three times for enabling the control action. The regeneration was done by changing CV mode to CC mode and increasing the current intensity. After 1 to 2 minutes, the PI controller was turned back to CV mode. While measuring the Coulombic efficiency, the heating of the cell to  $37^\circ\text{C}$  caused evaporation of water despite water vapour was fed to the suction side of the air blower. The Coulombic efficiency values (CE, %, based on two electrons transfer) and the specific energy values (SPEC,  $\text{Wh kg}^{-1}$  glucose) were calculated according to our earlier reported works [4-6]. Distilled water was added occasionally in the pumping vessel to compensate the evaporation of the aqueous electrolyte as it is described in our earlier work [6].

## 3. RESULTS AND DISCUSSION

### 3.1 Optimization of Pt and PtNi anode electrodes

When the total thicknesses of the PtNi(10 and 40 wt.%) anodes were compared in our earlier work [6], it was found that PtNi(10) with the thickness of  $700 \mu\text{m}$  gave better results than PtNi(40) with the thickness of  $460 \mu\text{m}$  although the ohmic and mass transport losses should be higher with the electrodes with the increased thicknesses. It was noted that the thicker electrode made from PtNi(10)

produced more effective active area on the catalyst layer for glucose oxidation reactions. The relevance of the catalysts with the high effective active areas has also been emphasized when the Raney platinum anodes were selected to be used in the fuel cells with glucose as a fuel [11]. The compositions of the anodes have been changed in this work. An additional porous carbon black (Vulcan XC-72) was blended with the catalyst-ionomer mixtures of the commercial PtNi(40) and Pt(60) that are both supported on carbon (designated PtNi(40) +C and Pt(60) +C). Using this procedure the thicknesses of the anodes were increased to 920 μm and 950 μm, respectively.

The values of OCV and current-voltage during the polarization tests with the modified anode electrodes are shown in Table 2. The reported values from our earlier work [6] as comparisons are also shown in Table 2. In all tests the cathode was the Pt(60), which had a thickness of 500 μm.

**Table 2.** The polarization data of the AEMFC with the modified Pt and PtNi anodes. The Pt cathodes were equal in both tests.

Anode catalyst [wt%]	OCV [mV]	Maximum current and end voltage [mA cm <sup>-2</sup> (mV)]
Pt(60)	605 [6]	0.70 (100) [6]
Pt(60) +C	587	0.39 (346)
PtNi(10)	420 [6]	0.24 (100) [6]
PtNi(40)	140 [6]	(NA) [6]
PtNi(40) +C	598	0.44 (370)

The polarization curves of the test fuel cell with PtNi (40) +C and Pt (60) +C anodes are shown also in Fig. 2.

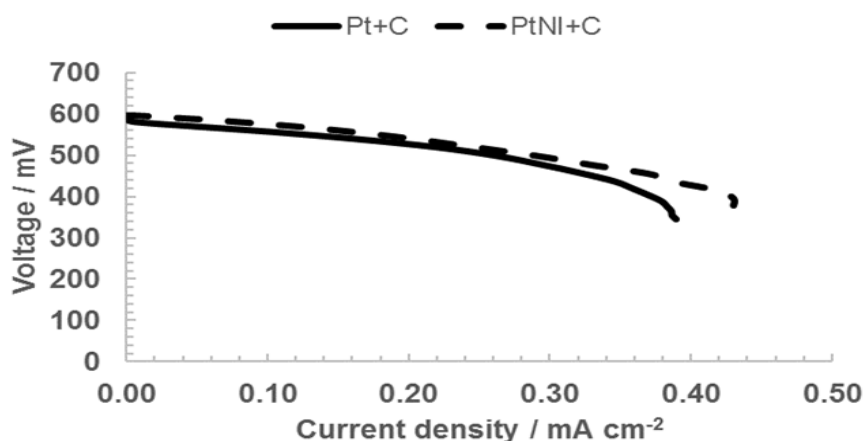


**Figure 2.** The polarization curve of the test fuel cell with modified PtNi(40) +C and Pt(60) +C as anodes.

Fig. 2 shows that both polarization curves are affected by high mass transfer losses already at around 0.4 mA cm<sup>-2</sup> and 0.4 V due to the high thicknesses of the modified PtNi(40) +C (920μm) and

Pt(60) +C (950  $\mu\text{m}$ ) anodes, so the minimum voltages of 100 mV were not achieved as in our earlier reported study [6]. However, the increase in the thicknesses of the anode electrodes improves both the OCV and current density values of the PtNi (40) +C electrode as an anode when compared to the PtNi(10) and PtNi(40) anode electrodes, whereas the modified anode electrode Pt (60) +C operated with slight OCV degradation than the thinner Pt(60) anode [6].

The measured and calculated data from the current-voltage test runs over time of the test fuel cell with the modified anode electrodes are shown in Table 3. The reported values from our earlier work [6] as comparisons are also shown in Table 3.

**Table 3.** Current-voltage values and calculated data of the direct glucose AEMFC with different Pt and PtNi anodes in this work and our earlier work in [6]. The Pt cathodes were similar in all the tests.

Anode catalyst (wt%)	Measured Coulombs $\sum \text{As}$	Average voltage [mV]	Average power [mWh]	Specific energy [ $\text{Wh kg}^{-1}$ ]	Coulombic efficiency [%/ 2 e-]
Pt (60) [6]	24.80	126	0.87	0.48	1.30
Pt (60) +C	24.59	184.5	1.26	0.64	1.16
PtNi (10) [6]	10.37	112	0.34	0.19	0.54
PtNi (40) +C	14.07	193.6	0.76	0.42	0.73

The results shown in Tables 2 and 3 show that the AEMFC with the PtNi(40)+C anode displays higher OCV, maximum current and Coulomb values than PtNi(10) as in Ref [6]. The maximum current density increased by 83.3% and the measured Coulombs increased by 35.7% when compared to tests with PtNi(10) in [6]. In regard to the modified Pt anode, the data in Tables 2 and 3 did not show any improvement compared to the thinner Pt(60) anode [6]. However, the data shown in Tables 2 to 3 were not optimal either for the modified PtNi(40)+C or the Pt(60)+C anodes, because the maximum current is already achieved at the voltage values of 370 mV and 346 mV with PtNi(40) + C and Pt(60)+C, respectively. By optimizing the electrodes, the amount of maximum current could possibly be increased and it could be reached at a lower potential, thus increasing the number of Coulombs gained from the system. The thicker electrodes cause higher ohmic losses and have lower diffusion properties compared to the thinner Pt(60) and PtNi(10) electrodes as mentioned in our earlier work [6]. The high thickness was also evident from slower equilibration during start-up: the durations for OCV generation were 3.5 and 1 hours for PtNi(40) +C and Pt(60) +C, respectively. The corresponding OCV generation times with thinner anodes were for PtNi(10) and Pt(60) 3 hours and 20 minutes, respectively [6].

The current-voltage tests in Table 3 show increased Coulombs with PtNi(40) +C compared to with the PtNi(10) anode [6]. Pt(60) +C did not produce higher measured Coulombs when compared to earlier results [6], but both the modified anodes produced higher average voltage and specific energy due to higher final voltage values. The Coulombs with PtNi(40) +C and Pt(60) +C could also have been much better if the voltage of the test fuel cell had been possible to run without interruption down

to the current of 20 to 30  $\mu\text{A}$  and the voltage of 100 mV as in [6]. Due to the high average power and general improvements, both of the modified anodes were selected to be used in the current-voltage measurement tests with the two-stage fuel cell system.. The PI electrical load was reprogrammed to be able to keep the test fuel cell in operation as long as possible with the thicker anodes.

### 3.2 Test of two stage direct glucose AEMFC system

The Coulombs for the two stage fuel cell systems were measured with the variation of PtNi(40) +C and Pt(60) +C anodes in both fuel cells. As comparison to detect the influence of the PtNi(40) +C anode in the fuel cell operation both fuel cells were run and measured with the modified Pt(60) +C anodes. The performance data and characteristics with the two-stage fuel cell system are shown in Tables 4 and 5.

**Table 4.** Performance data of the two-stage direct glucose AEMFC system with different anodes.. All fuel cells had similar standard Pt cathodes.

Anodes in FCs 1 & 2	Coulombs [As]	Average voltage [mV]	Average power [mWh]	Specific energy [Wh kg <sup>-1</sup> ]	Coulombic efficiency [% , 2e <sup>-</sup> ]
PtNi(40)+C & Pt(60) +C	21.50	213.00	1.27	0.64	1.01
Pt(60) +C & PtNi(40) +C	10.70	198.70	0.59	0.30	0.50
Pt(60)+C & Pt(60)+C	23.92	260.70	1.73	0.88	1.13

**Table 5.** The pH values of the fuel-electrolyte solutions before and after each current-voltage test of the two stage fuel cell system.

Anodes in FCs 1 & 2	Initial pH	Final pH value
PtNi(40) +C & Pt(60) +C	7.40	7.00
Pt(60) +C & PtNi(40)+C	7.40	7.20
Pt(60) +C & Pt(60) +C	7.40	7.10

The two stage fuel cell system with PtNi(40) +C as anode in FC-1 and Pt(60) +C as anode in FC-2 improved the Coulombs by 52.8% when compared to the single FC with PtNi(40) +C as anode (14.07 As, Table 3). Pt(60)+C in both of the FCs did not show improvement in the number of Coulombs (Table 4) when compared to the single FC with Pt(60) +C as anode (Table 3). It can be assumed that PtNi(40) +C with anodes in both the fuel cells would not yield higher yield in the number of Coulombs as shown in Table 3 and 4. Thus, no tests were conducted for the PtNi(40) +C and PtNi(40) +C with anodes at both fuel cells. However, higher average power and SPE (in Table 4) are

depicted for the two fuel cell systems than the single fuel cells systems (in Table 3). The SPE values of each fuel cell system are shown in Fig. 3.

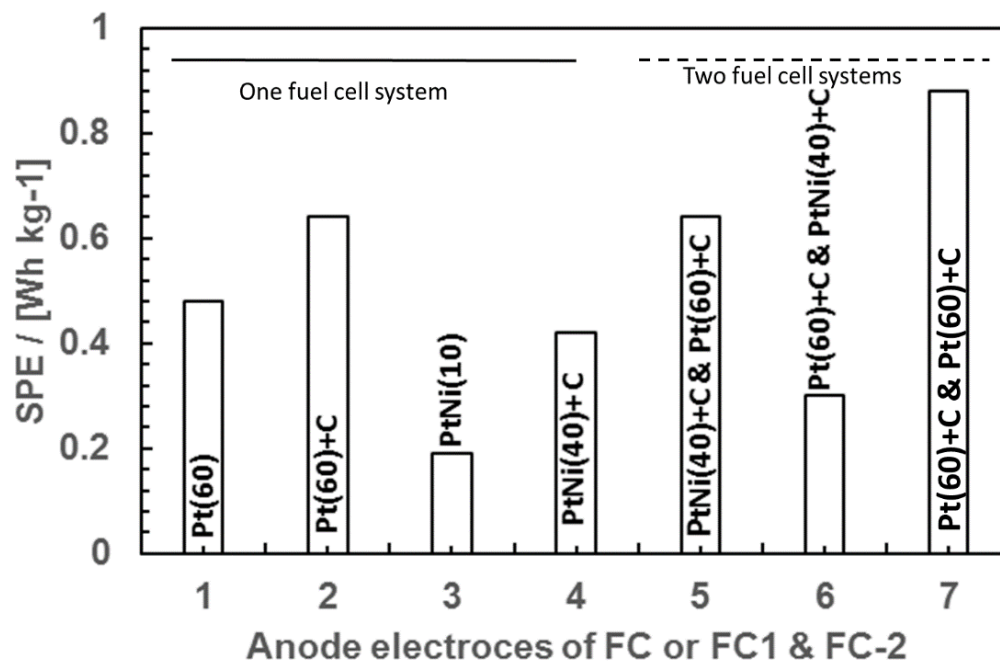


**Figure 3.** The specific energy (SPE) of each fuel cell system with one fuel cell and two fuel cells.

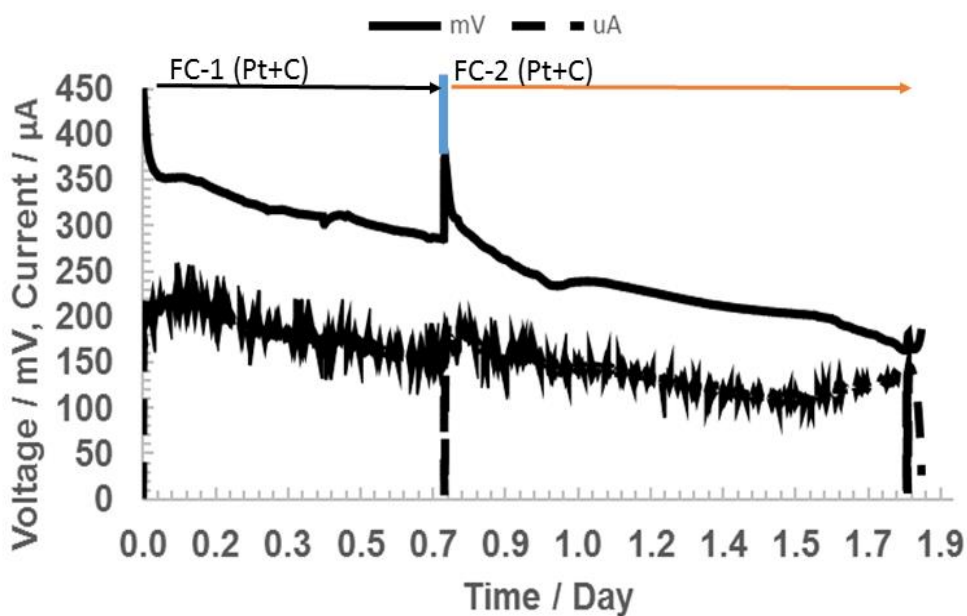


**Figure 4.** The current-voltage test for the two fuel cell systems with Pt(60) +C anodes in both fuel cells 1 and 2. The final voltage and current values remained above 100 mV and 20 – 30 µA, respectively. Change from FC-1 to FC-2 marked with blue line.

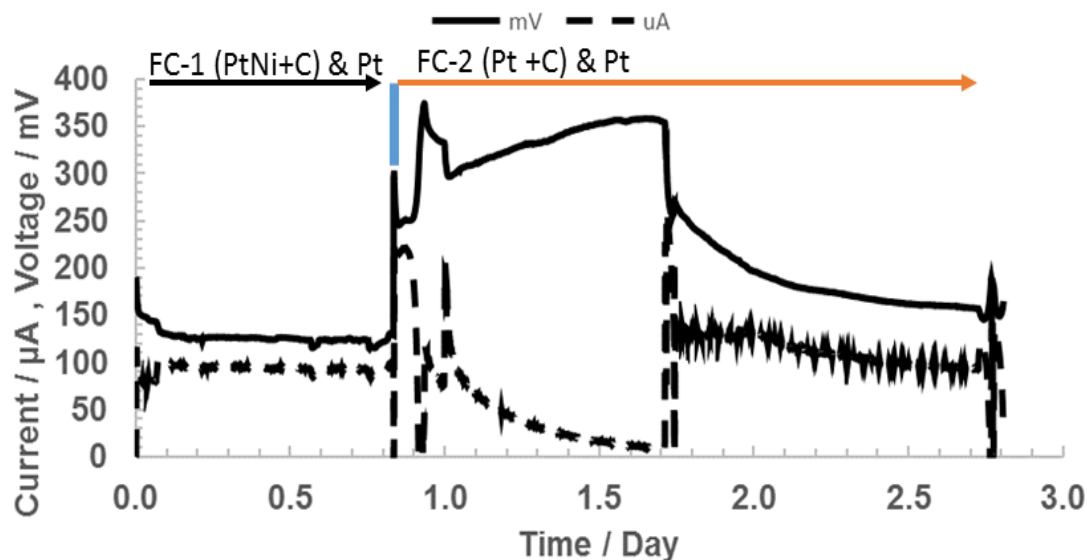


**Figure 5.** The current-voltage characteristics for the two-stage direct glucose AEMFC system with PtNi(40) +C and Pt(60) +C as anodes in fuel cells 1 and 2, respectively. The final voltage and current values remained above 100 mV and 20 – 30(150)  $\mu$ A, respectively. Change from FC-1 to FC-2 marked with blue line.

Fig. 3 shows that the best SPE value of the two fuel cell systems is based on Pt(60) +C & Pt(60) +C with more than 34% increase than the single fuel cell system. The PtNi(40) +C & Pt(60) +C as anodes show the biggest change in the pH value of the fuel-electrolyte solutions (Tabs 5). Thus, in the two stage fuel cell system inferior results on the average power and SPE were achieved when the selective and effective (on glucose molecule) anode catalyst (Pt(60) +C) was in the first fuel cell and the other anode catalyst (PtNi(40) +C) was in the later one. Figs. 4 and 5 show the two current-voltage measurements for the two stage fuel cell systems containing the two different electrocatalyst compositions.

In all the tests with the thick anode formulations, the voltage of the last fuel cell FC-2 did not reach the final voltage of 100 mV and final current between 20 – 30  $\mu$ A as in earlier tests with thinner anodes due to higher diffusion and ohmic losses [6]. Thus, there remained a lot of unused potential in the glucose-electrolyte solution to be electro-oxidized with a higher number of extracted Coulombs. The two-stage oxidation process should be repeated in fuel cells with better physical properties (i.e. higher surface areas, chemical and morphological properties of the catalysts as well as structures of the electrodes). There is also a need to improve and develop the control unit of the electronic load so that much lower values of both voltages and currents are obtained to perform in steady state

In Fig. 4, it is shown that the voltage of the fuel cell decreases steadily with Pt (60 wt.%) anodes in both the fuel cells. Whereas, it is shown in Fig. 5 that the PI controlled electric load could not keep the current steady in FC-2 with the Pt(60) +C anode but medium manual control actions had to be done to regenerate the control capacity of the electrical load. The electrocatalysts in FC-2 were activated very slowly, which could be shown in Fig. 5, where an increase in the voltage of the fuel cell during the first hour from the start-up was noticeable. Thus, it could be observed that the PI electronic

load with PI controller demanded the regeneration of the PI control capacity three times during the test when PtNi(40) +C and Pt(60) +C were used as anodes, whereas with Pt(60) +C as anodes (Fig. 4) the regeneration was done only two times at the end of the test.

As for the oxidation products from the glucose electrochemical oxidation; they were not analysed due to the low Coulombic efficiency values shown in Tab. 4. From the literature, it can be concluded that the main oxidation product with Pt-derived anode electrodes is gluconic acid, but also glucuronic, glucaric, oxalic and tartaric acids can be formed [12,13]. Very small amounts of glycolic and formic acids have been detected as well [12]. The measured pH-values in this work (Tab 5) are lower than the final pH values were for the cylinder shaped fuel cell with different concentrations of the fuel-electrolyte solutions tested in the temperature range from 20 to 37°C [4-5]. This indicates increased formation of acidic oxidation products in the liquid phase as a result of the electrochemical oxidation of glucose. Thus, from the results shown in Tables 4 and 5 it is possible to assume that by using the multi stage direct glucose fuel cell system it could be possible to achieve a higher specific energy values. To this end, more selective and active anode catalysts than those used here or earlier [4-6] are sought for the electro-oxidation of glucose and its intermediate products.

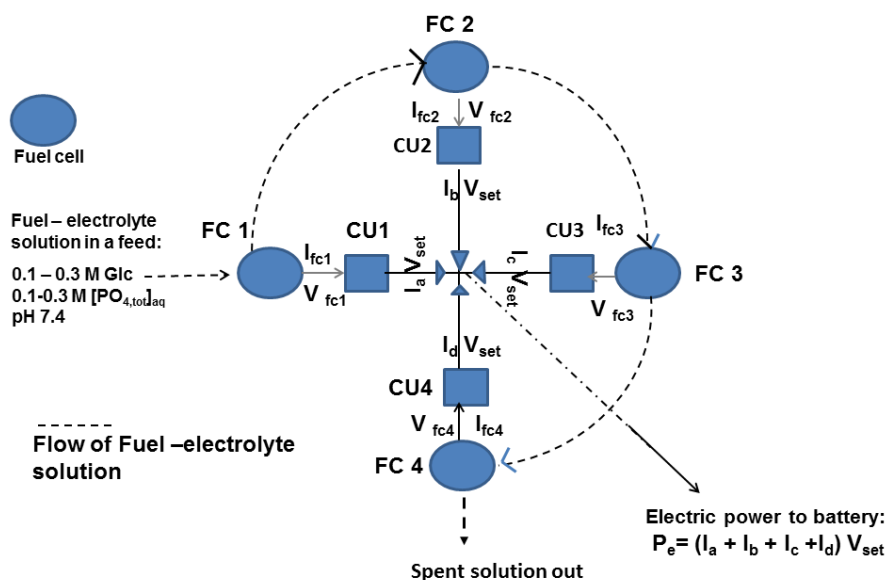


**Figure 6.** The principle flow sheet for a multistage fuel cell system as a charger of a battery, which contains four fuel cells. Each fuel cell (FC) has its own control and transformer unit (CU). The oxidation of glucose occurs step by step in each fuel cell. The fuel cells have different electrocatalysts for glucose and its oxidation products.

The development of an effective multistage direct glucose fuel cell system have to contain an effective control system with load variations for the oxidation process itself and maintaining the pH of the fuel-electrolyte constant or near the starting value. Glucose is reported to be unreactive when the fuel-electrolyte solution turns to be acidic [12]. If necessary, additional energy in the form of high frequency signals with certain voltage level should be fed into each fuel cell as has been done earlier with alkaline glucose fuel cells [14-15]. Another strategy might be adding certain chemicals into the

fuel-electrolyte solution to cause chemical reforming or corresponding reactions to expose the glucose to be more reactive for the electro-oxidation. Overall, the prerequisites for a higher degree of glucose oxidation by abiotic fuel cells can be effective compared to the multi enzymatic Krebs cycle in living cells, in which glucose is used to produce different compounds [16]. The success of the effective electro-oxidation of glucose will be the sum of multidisciplinary factors, which have not been taken into account so far. The principal flow sheet of the multistage fuel cell system to be as a battery charger is shown in Figure 6.

#### 4. CONCLUSIONS

Anode catalysts Pt(60) and PtNi(40) were assembled in electrode configurations by increasing their thicknesses through addition of carbon for the oxidation reactions of glucose. These modified anodes were tested at first in AEMFC. The improvements in the current densities-voltages were noticed especially for PtNi. Both the catalysts were also used in the two-stage AEMFC system to compare with the single fuel cells with similar anodes. The current-voltage tests showed that the number of Coulombs were very close to the values with the single fuel cells, but glucose remained to some extent unoxidized giving rise to low efficiency. The measurements showed that in the two-stage fuel cell system with the anode (PtNi) in the first stage and the selective anode (Pt) in the last stage produced the highest relative improvement compared to the single fuel cell with PtNi as anode. Furthermore, Pt+C & Pt +C showed by far greatest average power (mWh) and specific energy (SPE). Thus, increasing the number of the fuel cells from one to two pieces increased the average power of the extracted current from the glucose electrochemical oxidation. After the searching more effective electro catalysts for the fuel cells, it is expected that the improvement in both the extracted Coulombs together with the average power are expected to be attained by means of the multistage direct glucose fuel cell systems.

#### ACNOWLEDGEMENTS

This research was financially supported by Jane & Aatos Erkko Foundation.

#### References

1. Ó. Santiago, E. Navarro, M. A. Raso and T. J. Leo, *Appl. Energy* 179 (2016) 497.
2. S. Kerzenmacher, J. Ducreé, R. Zengerle and F. von Stetten, *J. Power Sources* 182 (2008) 1.
3. N. Mano, F. Mao and A. Heller, *J. AM. Chem. Soc.* 125 (2003) 6588.
4. J.-P. Spets, M. J. Lampinen, Y. Kiros, J. Rantanen and T. Anttila, *Int. J. Electrochem. Sci.*, 7 (2012) 11696.
5. J.-P. Spets, M. J. Lampinen, Y. Kiros, J. Rantanen, T. Anttila, *Int. J. Electrochem Sci*, 8 (2013) 1226.
6. J.-P. Spets, P. Kanninen, T. Kallio, J. Selkänaho, Y. Kiros, K. Saari and M. Larmi, *Int. J. Electrochem. Sci.*, 11 (2016) 4219.
7. I. Beceric and F. Kadirgan, *Synthetic Metals*, 124 (2001) 379.
8. A. Brouzgou and P. Tsiakaras, *Top. Catal.*, 58 (2015) 1311.

9. P. Aelterman, K. Rabaey, H. T. Pham, N. Boon and W. Verstraete, *Environ Sci. Technol.* 40 (2006) 3388.
10. S. Elangovan, A. C. Khandkar and J. J. Hartvigsen, U.S Patent 5,480,738 (1996) USA.
11. B. I. Rapoport, J. T. Kedzierski and R. Sapeshkar, *PLoS ONE*, 7 (2012) e38436.
12. K. B. Kokoh, J.-M. Léger, B. Beden and C. Lamy, *Electrochim. Acta* 37 (1992) 1333.
13. A. Abbadi and H. van Bekkum, *J. Mol. Cat. A: Chem.*, 97 (1995) 111.
14. J-P. Spets, M. J. Lampinen, Y. Kiros, T. Anttila, J. Rantanen and T. Granström, *Int. J. Electrochem. Sci.*, 5 (2010) 547.
15. J-P. Spets, M. A. Kuosa, Y. Kiros, T. Anttila, J. Rantanen, M.J. Lampinen and K. Saari, *J. Power Sources*, 195 (2010) 475.
16. H. Hart, R. D. Schuetz, Organic Chemistry, 5th Ed, Houghton Mifflin, ISBN 0-395-26492-8, (1978) USA.

© 2017 The Authors. Published by ESG ([www.electrochemsci.org](http://www.electrochemsci.org)). This article is an open access article distributed under the terms and conditions of the Creative Commons Attribution license (<http://creativecommons.org/licenses/by/4.0/>).